THE ASTROPHYSICAL JOURNAL, 227:808–815, 1979 February 1

OBSERVATIONS OF THE DIFFUSE INTERSTELLAR EUV RADIATION FIELD

B. R. SANDEL
Lunar and Planetary Laboratory, University of Arizona
D. E. SHEMANSKY
Lunar and Planetary Laboratory, University of Arizona
AND
A. LYLE BROADFOOT
Kitt Peak National Observatory*
Received 1978 May 23; accepted 1978 August 15

ABSTRACT

The diffuse interstellar EUV spectrum in the wavelength range 750–1200 Å has been measured for the first time with the *Voyager* ultraviolet spectrometers. A spectral half-width of 30 Å was obtained. Measurements in several directions show intensities at 975 Å ranging from a maximum of about 1×10^{-7} ergs cm^{-2} s^{-1} sr^{-1} Å^{-1} near the galactic plane to an upper limit of about 1×10^{-8} ergs cm^{-2} s^{-1} sr^{-1} Å^{-1}. Preliminary analysis suggests that some theoretical predictions of the interstellar EUV intensity are in fairly good agreement with these measurements.

Subject headings: interstellar: abundances — interstellar: matter — ultraviolet: spectra

I. INTRODUCTION

The diffuse EUV radiation field in interplanetary space is expected to include contributions from several sources. A local component is due to resonant scattering of sunlight by the nearby interstellar medium. There is expected to be diffuse emission arising within the Galaxy, and perhaps an extragalactic component as well. The galactic emission and extragalactic emission are referred to as the interstellar EUV radiation here.

Observations of the interstellar EUV radiation are of interest from several points of view. The galactic component of this radiation field may play an important part in the ionization of the interstellar medium (Hill and Silk 1975). Furthermore, the discovery and measurement of an extragalactic component would be an important contribution toward dealing with the questions of the existence and characteristics of an intergalactic medium. Predictions of the galactic EUV radiation field have been developed by Grewing (1975), Jura (1974), Gondhalekar and Wilson (1975), and others. Recently Henry (1977) performed integrations of light from catalogued stars to arrive at predictions of the spatial variation of the galactic UV brightness. A useful review of measurements of UV sky brightness has been prepared by Davidsen, Bowyer, and Lampton (1974). This review emphasizes the wide variations in early experimental data. In part these variations are due to large differences in the size of the field of view of the various instruments used, resulting in varying contributions from hot stars included in the field. With the exception of a recent measurement by Paresce and Bowyer (1976), no data are available shortward of the MgF_2 cutoff at 1050 Å. Their measurement was made with 40 Å spectral half-width over a range of 775–1050 Å. Since terrestrial airglow could not be ruled out as the source of the observed radiation, it was possible only to place upper limits on the extraterrestrial intensity.

We report here the first observations and preliminary analysis of the diffuse EUV radiation field showing positive measurable fluxes in the wavelength range 912–1200 Å. These observations were made with ultraviolet spectrometers (UVS) on the two *Voyager* spacecraft. Since contamination by terrestrial airglow was absent, and the small field of view permitted the effective exclusion of hot stars from the regions of observation, two major problems commonly encountered by other experiments have been eliminated.

II. INSTRUMENT AND OBSERVATIONS

Each *Voyager* ultraviolet spectrometer is an objective-grating spectrometer covering the wavelength range of approximately 500–1700 Å in 128 contiguous intervals. A complete description of the instrument may be found in Broadfoot *et al.* (1977). Radiation passing through the open mechanical collimator to the concave grating is dispersed and focused on the photoelectron counting detector. Here the photon image is converted by a microchannel plate electron multiplier followed by a linear 128-element self-scanned anode array for signal readout (Broadfoot and Sandel 1977). A CuI photocathode deposited on a MgF_2 filter overlaps the 1250–1700 Å portion of the detector to enhance the quantum efficiency over that of the bare microchannel plate. The field of view of the primary aperture is a slit with a triangular trans-

* The Kitt Peak National Observatory is operated by the Association of Universities for Research in Astronomy, Inc., under contract with the National Science Foundation.

mission function of 0°.1 half-width in the direction of dispersion and a length limited to 0°.86 in the cross-dispersion direction. The collecting area for the primary aperture is 21.2 cm^2. An auxiliary aperture has an area of 0.78 cm^2 and a field of view of 0°.3 FWHM × 0°.86. The view direction of this field, which will be used to observe the Sun, is offset by 20° from the primary field. Since both apertures are open continuously, the position of the auxiliary field must be taken into account when making observations with the primary field. The ratio of the throughput of the primary to the occultation apertures is 8 and 20 for extended and point sources, respectively.

The observations discussed in this report were obtained during the normal course of operation of the *Voyager* spacecraft in interplanetary cruise. From time to time during the mission, the position of the spacecraft scan platform, on which the UVS is mounted, remained fixed for several days. Therefore the long integration periods required to measure extremely low-level signals with an instrument having a small field of view and a relatively small grating area are available. During these periods, the field of view of the UVS moved about 0°.25 day^{-1} over the celestial sphere due to the motion of the spacecraft along its trajectory. Superposed on this drift was a periodic motion arising from the spacecraft attitude control. This "limit-cycle" motion had an amplitude of about ±0°.5 and a period of about 40 minutes. Thus a star near the mean view direction moved in and out of the UVS field because of the limit-cycle motion.

Of the many drift sequences executed since launch of the two spacecraft in 1977 August and September, 10 have been selected as suitable for analysis for cosmic EUV emissions. Pertinent characteristics of these 10 drifts are summarized in Table 1. The primary reason for excluding other drifts having sufficient integration time in a particular direction was the presence of stars in the spectrometer field of view. Since these observing sequences were not designed specifically for diffuse EUV measurements, the distribution of observations over the celestial sphere is less than optimum. Nevertheless, a range of view directions are available sufficient to provide valuable new information.

III. ANALYSIS

A typical spectrum is shown in Figures 1*a* and 1*b*. The most prominent aspects of this spectrum are lines at H Lα, H Lβ, and He 584 Å due to resonant scattering of bright solar lines by the neutral hydrogen and helium of the interstellar medium. This first measurement of resonantly scattered H Lβ from the interstellar medium has been discussed by Sandel, Shemansky, and Broadfoot (1978) and Shemansky, Sandel, and Broadfoot (1978). At other wavelengths are measurable signals which result from a combination of internal scattering of the bright lines (primarily H Lα) into other channels, cosmic-ray noise, thermal noise in the microchannel plates, and, in other spectra, diffuse interstellar EUV radiation. Figure 2 shows a similar spectrum taken in a different direction which is interpreted in the following discussion as a measurement of the interstellar radiation field between 912 and 1150 Å.

A quantitative analysis of these spectral data requires that: (1) cosmic-ray and thermal noise be eliminated; (2) internal scattering from bright lines be eliminated; and (3) the possibility of a contribution to the signal from direct starlight be ruled out, as far as possible.

1. *Cosmic-ray and thermal noise.*—Direct measures of the apparent spectral content and magnitudes of these sources have been obtained from solar flare activity and from observations of the optical calibration plate mounted on the spacecraft. The calibration plate serves as an effective dark slide for the UV spectrometer (Shemansky *et al.*), although there is some weak contribution from reflected 1216 Å emission. Apart from differences in threshold correction, the cosmic-ray signal is constant over the wavelength scale with a step function at the edge of the filter photocathode. Figure 1*c* shows the spectrum of Figures 1*a* and 1*b* after subtraction of the noise spectrum. There is some uncertainty in the magnitude

TABLE 1

SUMMARY OF THE OBSERVATIONS

Observation	*Voyager*	Integration Time (s)	View Direction: Equatorial Coordinates α	Equatorial Coordinates δ	Galactic Coordinates l^{II}	Galactic Coordinates b^{II}	Flux at 975 Å 10^{-8} ergs (cm^2 s sr Å)$^{-1}$
A	2	2.71E5	74	+18	183	−14	6.2 ± 0.3
B	2	2.01E5	54	−7	162	−21	< 1.0
C	2	5.01E5	317	−26	22	−42	Background
D	1	4.32E5	100	−11	222	−7	5.7 ± 0.4
E	1	1.71E5	108	+13	205	+12	9.1 ± 0.5
F	1	2.16E4	112	−14	230	+3	9.5 ± 0.9
G	1	3.74E4	141	+16	216	+42	< 1.4
H	1	1.18E5	78	+19	185	−11	4.4 ± 0.5
J	1	7.46E4	106	+80	134	+28	< 1.4
K	1	1.27E5	46	+30	155	−24	Background

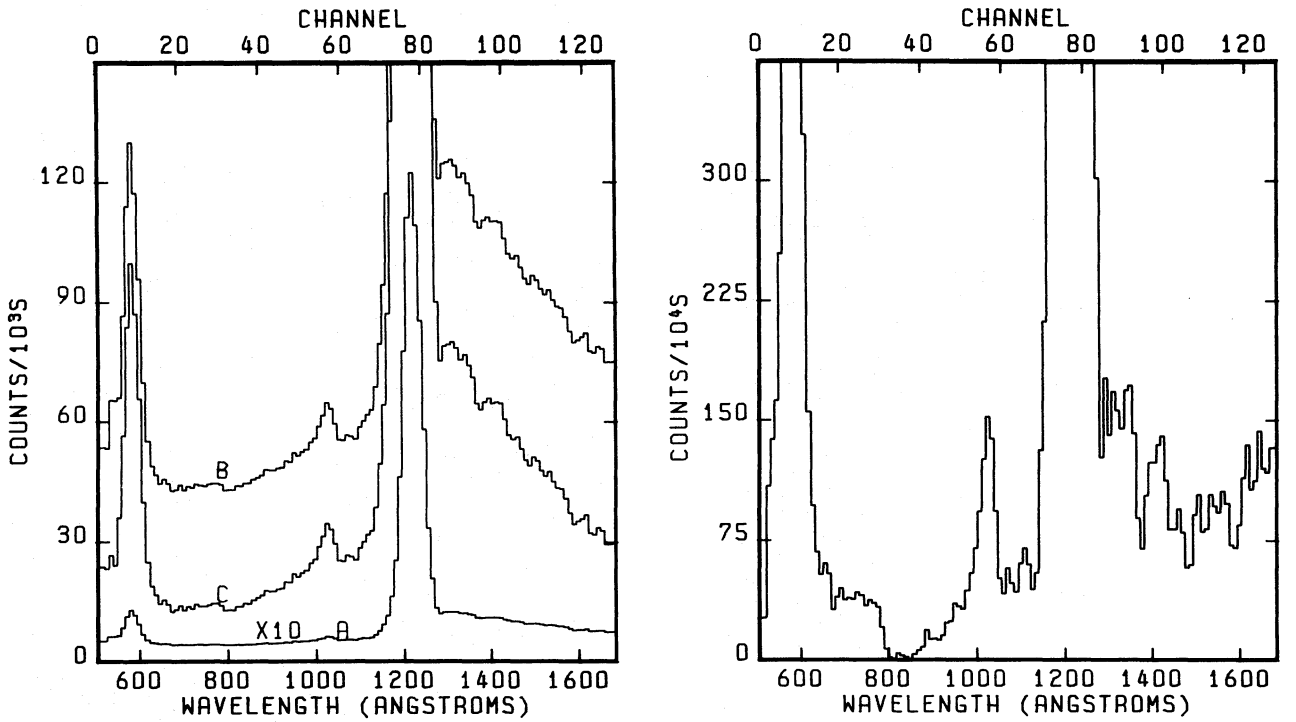

FIG. 1.—*Voyager 2* UV spectrum of the interstellar medium in the mean direction α 317°, δ −26° (1950). The spectrum, judged to be the least complex of the interstellar medium spectra, is dominated by the emission lines He 584 Å, H Lβ 1026 Å, and H Lα 1216 Å. The apparent continuum is due to internal instrumental scattering of the observed lines, thermal and cosmic-ray noise, and some measurable interstellar medium emission. The integration time is 5×10^5 s. The data are scaled to counts per 1000 s and may be compared directly with Fig. 2. This spectrum corresponds to observation *C* in Table 1. (*a*) Raw data corrected only for variation in threshold response of the anode detectors, scaled down by a factor of 10 relative to the ordinate scale. (*b*) Same as (*a*), but scaled to the ordinate numbers. (*c*) The data of (*b*) after subtraction of cosmic-ray noise determined from observation of the spacecraft calibration plate (see text). (*d*) The spectrum of (*c*) after multiplication by a low-resolution scattering matrix, designed to remove the internal instrumental scattering component. This resultant spectrum is judged to be dominated by real emission features.

of the subtracted spectrum due to possible variations in normal solar activity, but the amount subtracted to produce Figure 1*c* is the measured rate observed during the calibration plate observations. Comparison of Figures 1*b* and 1*c* shows that the noise background accounts for about 70% of the apparent continuum signal at ~700 Å and about 50% of that at 1600 Å. The statistical uncertainty in the remaining signal (Fig. 1*c*) at 700 Å and 1600 Å is ±7% and ±4.5%, respectively. The results for the other spectra examined here are similar. The remaining signal represented by Figure 1*c* is thus estimated to be due only to the dispersion and scattering of photons passing through the entrance aperture.

2. *Internal instrumental scattering.*—Each spectral element of the incoming radiation produces a characteristic scattering spectrum in the instrumental signal. The magnitude of this signal falling outside of the instrumental resolution function ultimately limits the dynamic range of the instrument. The scattering characteristics of the *Voyager* instruments have been measured during preflight laboratory calibration. Scattering matrices based on the laboratory data are being developed which can be used to remove the scattered component from the observed signal. The dominant scattered signal in the interstellar medium spectra is due to the very bright 1216 Å hydrogen line. Figure 1*d* shows the spectrum of Figure 1*c* after removal of the scattered components. The statistical uncertainty in the remaining signals at 700 Å and 1600 Å after removal of the scattered component is approximately ±30% and ±10%, respectively. The analysis thus seems to suggest measurable residual signals at wavelengths other than He 584 Å, Lβ 1026 Å, and Lα 1216 Å radiation. The question then is whether the residual signal is due to inaccuracy in the scattering analysis and simply represents the scattered residue of Lα, or whether it is real and independent of Lα. Our conclusion on the basis of this primary analysis is that the signal is real. However, we confine ourselves in this paper to the 912–1150 Å region where well-defined variations are observed as a function of observational direction. Scattering matrices are not yet available for *Voyager 1* data, and a more complete analysis of the entire spectrum must await a complete set of analyzed data of the kind shown in Figure 1*d*. In order to obtain a more complete set of data in the short-wavelength region, the spectrum of Figure 1 and another spectrum obtained from the *Voyager 1* instrument were used as reference spectra for observations in other directions,

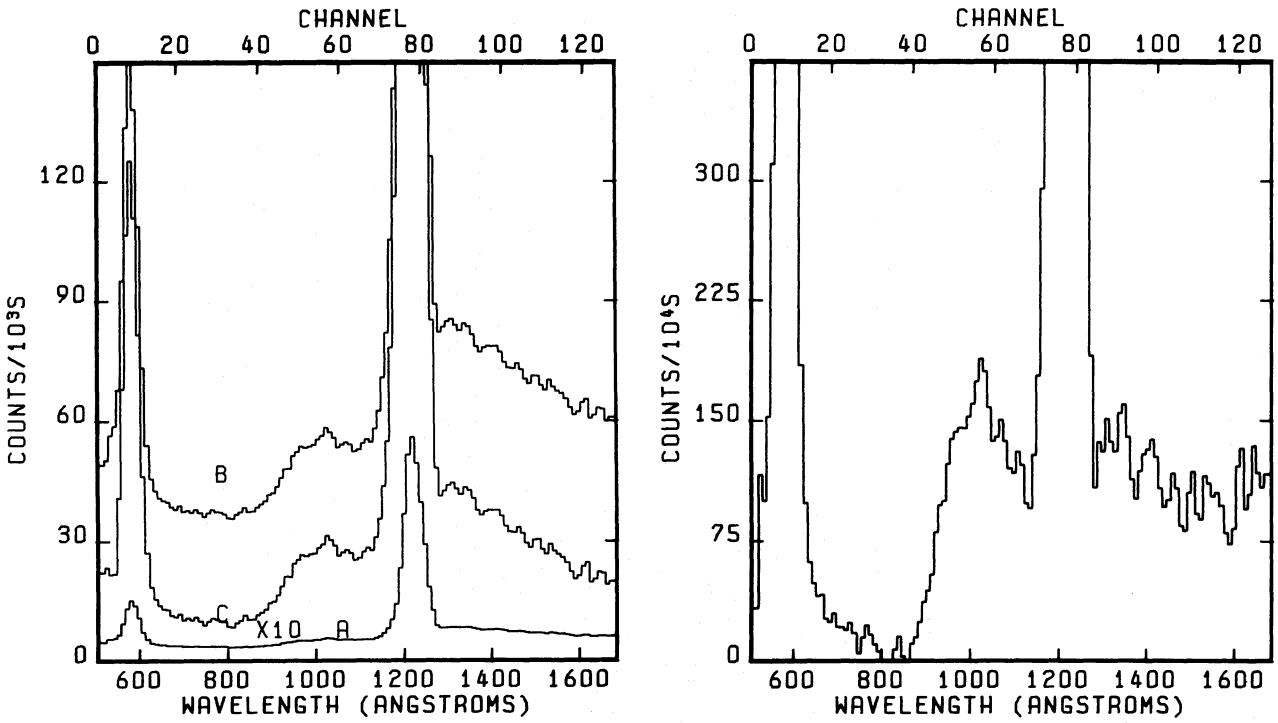

FIG. 2.—A *Voyager 2* spectrum showing strong evidence of diffuse EUV radiation with a distinct edge in the vicinity of 912 Å. The signal in the 900–1150 Å region is clearly enhanced over that of Fig. 1. Note that the 1216 Å and 1026 Å features in this spectrum are reduced by more than a factor of 2 relative to Fig. 1. The integration time is 2.714×10^5 s. This spectrum corresponds to observation *A* in Table 1. (*a*, *b*, *c*) are equivalent to those shown in Figs. 1*a*, *b*, *c*. (*d*) The spectrum of (*c*) after removal of internal instrumental scattering as described in Fig. 1*d*.

since the spectral content appeared to be the least complicated of the observed spectra. The observational directions of both of these reference spectra are in regions of the celestial sphere for which an extremely low galactic EUV brightness is expected on the basis of calculations by Henry (1977).

3. *Elimination of direct stellar contributions.*—The small UVS field of view (2.6×10^{-5} sr) facilitates the exclusion of hot stars from the field, giving the UVS an important advantage over most earlier experiments to measure the diffuse EUV emission. Several techniques have been used to exclude observations having stars in the field of view for a part of the integration time. First, sufficiently bright stars have a characteristic spectral signature and move in and out of the field of view in a predictable way. These are easy to exclude from the data. To eliminate signals from stars not bright enough to produce an obvious increase in count rate, other methods may be used. The track of the view direction across the celestial sphere, which is known absolutely to about 0°.2, has been compared with a map of the sky generated by using cataloged bright stars and their color indices (Henry 1977). With this information, data taken near stars bright enough to contaminate the measurement can be rejected. Finally, spatial binning of the data in which spectra were accumulated for a specific look direction has shown conclusively that the emission measured here was spatially extended rather than from a point source. We are therefore confident that these data show a significant emission of diffuse origin.

a) Spectral Characteristics

The distinct difference in the spectral shape of Figures 2*a* and 2*b* from that of Figures 1*a* and 1*b* in the 912–1150 Å region goes beyond any question concerning the scattering contribution of 1216 Å radiation. It indicates the presence of a signal of spatially diffuse origin. The spectrum of Figures 2*a* and 2*b* has been analyzed in the same manner as that of Figures 1*a* and 1*b*, and Figure 2*d* shows the spectrum after removal of internal scattering. Other important distinguishing features of these two spectra are the differences in brightness of the line features. The Lα 1216 Å and Lβ 1026 Å lines of Figure 1*d* are more than a factor of 2 brighter than those of Figure 2*d*, whereas the He 584 Å line is less bright by a factor of 1.3 in the same frame of reference. The spectra in the 1250–1680 Å region have a very similar spectral content and almost the same absolute brightness, demonstrating their independence of the 1216 Å radiation. The signal at 975 Å in Figure 2*d* is a factor of 5 greater than that of Figure 1*d*.

The spectrum of Figures 1*a* and 1*b* can be used as a "scattering background" spectrum to obtain results in the 912–1150 Å region equivalent to the analysis process resulting in Figure 2*d*. The reason for this is

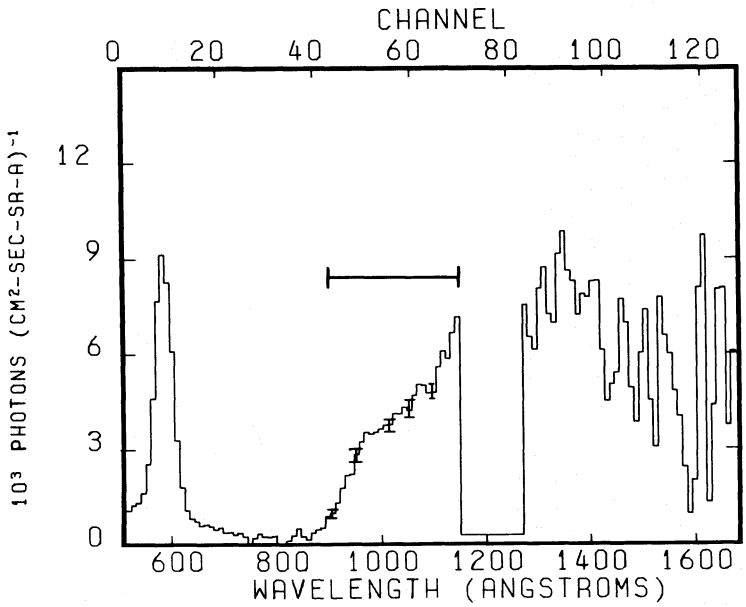

FIG. 3.—This spectrum is the result of subtracting the local emission and its scattering products scaled from Fig. 1 from the spectrum in Fig. 2. Error bars indicate the $\pm 1\ \sigma$ statistical uncertainty for several points. Inferences about the interstellar EUV radiation have been drawn only from the wavelength range 750–1150 Å. The horizontal bar shows the spectral range in which a positive signal has been analyzed in this work. The large residual He 584 signal results from the fact that the ratios of the intensities of the local He 584 and H 1216 emissions are not the same in observations *A* and *C*. This residual has no bearing on the intensity in this wavelength band. The large statistical uncertainty longward of 1250 Å reflects the fact that the instrument sensitivity is lower in this region. The signal in this figure differs from that of Fig. 2*d* in that the 1026 Å and 1216 Å features have been removed by the analysis procedure and the signal levels have been depressed due to the presence of measurable signals in the "background" spectrum (see Fig. 4).

clear on visual comparison of Figures 1 and 2. Figure 3 shows the spectrum of Figures 2*a* and 2*b* after subtraction of the spectrum of Figures 1*a* and 1*b* scaled to the same Lα intensity. Figure 4 shows the spectrum of Figure 2*d* on an absolute scale, for direct comparison with Figure 3. The analysis process resulting in Figure 3 thus produces an underestimate of EUV emission rate by about 30% at 975 Å and by about a factor of 2 in the 1250–1680 Å region, if we use the scattering matrix analysis (Fig. 4) as a reference. The remaining spectra discussed here have been analyzed by using the spectrum of Figures 1*a* and 1*b* and a comparable spectrum from the *Voyager 1* instrument as "scattering background" spectra in lieu of a full analysis with scattering matrices, to obtain a measure of the interstellar EUV radiation in the 912–1150 Å region. These scattering background spectra do contain a contribution from the EUV interstellar radiation, according to our analysis, and the effect is an underestimate of the fluxes in these measurements. Since the dominant source of scattering contamination is the H Lα line, the scattering background spectrum was scaled to an integrated Lα intensity equal to that in the data spectrum, and then subtracted from the data. Cosmic-ray and thermal noise were first removed from both spectra. Of course, information on the diffuse EUV intensity at wavelengths near Lα is lost in this process. At wavelengths greater than 1250 Å, the CuI photocathode is more sensitive to scattered Lα than the bare microchannel plate at shorter wavelengths. The sensitivity is also low compared to the 600–1200 Å region (see Fig. 7).

The spectral characteristics of all the spectra having a measurable diffuse EUV component in the 912–1150 Å region are similar to those shown in Figures 2*a* and 2*b*. The results of all observations are summarized in Table 1. In the case of three of these, no measurable signal was present above the background reference spectra, and upper limits have been assigned.

IV. DISCUSSION

The present measurements are compared with various theoretical predictions and previous measurements in Figure 5. The predictions are based on assumptions of the general characteristics of the interstellar medium and of the spectra and spatial distribution of hot stars. Some of these predictions include variations with galactic latitude, but the only calculation of higher spatial resolution is that of Henry (1977), discussed later. Spectral characteristics and absolute intensities of several of the predictions are in reasonable agreement with the present measurements, in view of the possibility of longitude variations not included in the theories. Except for measurements at high galactic latitudes made by Henry, previous measurements indicate higher fluxes than measured here. This may be because the larger fields of view made earlier measurements more subject to contamination by

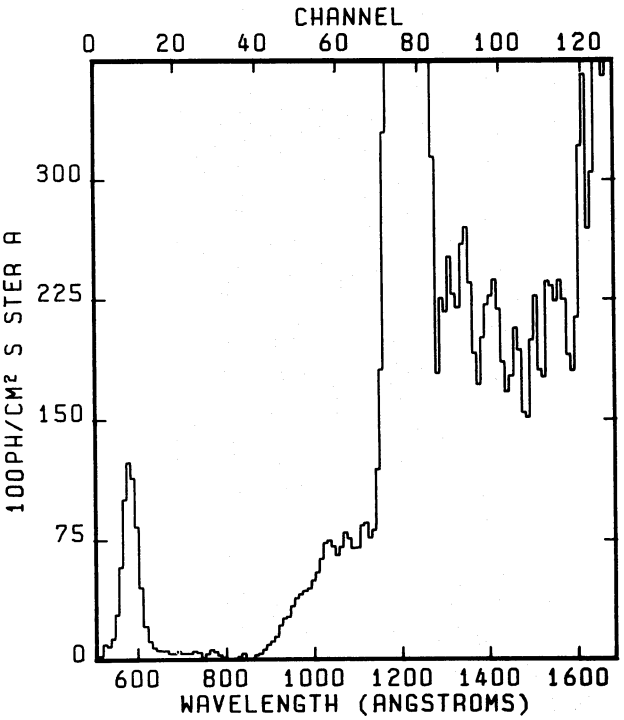

FIG. 4.—The spectrum of Fig. 2*d* on an absolute scale for direct comparison with Fig. 3. The relative spectral response of the instrument is shown in Fig. 7.

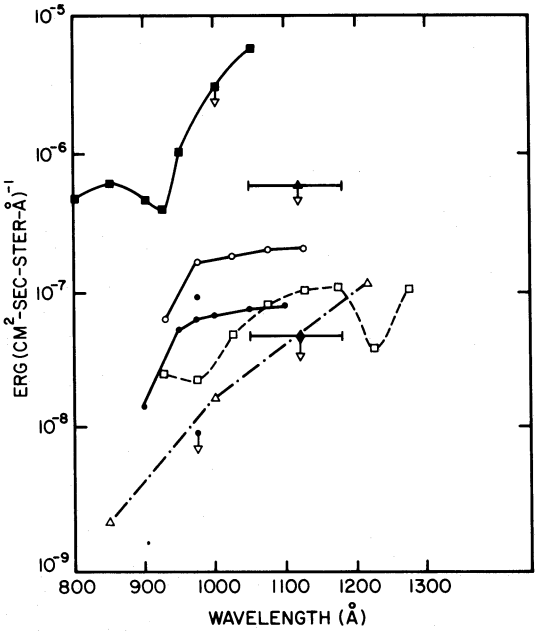

FIG. 5.—A comparison of this measurement (*solid line*) with other measurements (*solid symbols*) and theoretical calculations (*open symbols*). The typical spectrum as well as maximum signal and minimum upper limit at 975 Å found in this work are indicated by solid circles. Other experimental data are those of (*solid squares*) Paresce and Bowyer (1976), (*solid triangle*) Belyaev *et al.* (1970), and (*solid diamond*) Henry (1973). Calculations shown are those of (*open circles*) Jura (1974), (*open squares*) Gondhalekar and Wilson (1975), and (*open triangles*) Grewing (1975). The three earlier experiments shown here yielded upper limits only, although positive measurements at longer wavelengths have been made (e.g., Henry *et al.* 1977 and Hayakawa *et al.* 1969). The bandpass of photometer experiments is indicated by a horizontal line. The upper limit of Henry does not conflict with the present measurement, since it was made at high galactic latitude where the galactic EUV component should be minimal.

direct starlight. The present measurements are easily compatible with the upper limits placed by Paresce and Bowyer (1976), falling one to two orders of magnitude below their limits.

The only prediction including a directional variation of the sky background intensity other than with latitude is that of Henry (1977) based on summation of cataloged stars. Our measurements at 975 Å are compared with Henry's calculations in Figure 6. Differences in specific directions are as much as an order of magnitude; this is undoubtedly because Henry's calculations represent integrations over relatively large portions of the celestial sphere (approximately 100 square degrees), whereas the UVS sampled a much smaller area (typically 5 square degrees). In some cases Henry's calculations include bright stars are are excluded from our field of view.

In two (observations *G* and *J*) of the three directions in which our measurements provide only upper limits, the brightness calculated by Henry is two orders of magnitude or more below the limit placed here. In the third direction (observation *B*), the calculated intensity is about the same as the upper limit inferred from this measurement.

Also shown in Figure 6 is a calculation by Gondhalekar and Wilson (1975) of the variation with galactic latitude of radiation in the 975–1025 Å band. It is apparent that the intensities measured here fall off much more rapidly with increasing distance from the galactic plane than is predicted by this calculation, which includes contributions from both stars and scattered light. However, the rapid falloff may be partly due to our use of the "scattering background" spectra in the analysis. The "background" spectrum used for the *Voyager 2* data shown in Figure 1*d* after scattering analysis actually indicates an emission rate of 1.6×10^{-8} ergs (cm^2 s sr Å)$^{-1}$ at 975 Å. This is still somewhat below the Gondhalekar and Wilson (1975) curve, but shows much better agreement.

The shape of the interstellar EUV spectrum in the 912 Å region is of considerable interest in that we can make inferences from it concerning the amount of neutral hydrogen in the near vicinity of the solar system (Grewing 1975). The lack of measurable emission in the 800–875 Å region appears to be a characteristic of the spectra obtained here, including the "background" spectrum of Figure 1*d*. The signal appears to rise toward longer wavelengths beginning at about 875 Å ± 10 Å. This indicates that the spectral intensity begins to rise significantly in the vicinity of 912 Å. The signal rises steeply, but not limited by spectral resolution, to

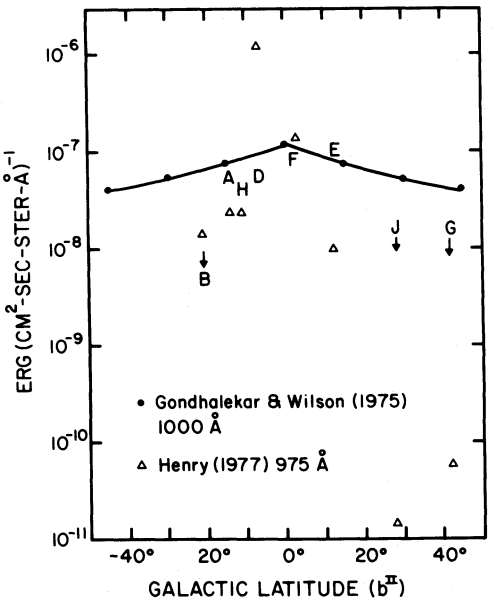

FIG. 6.—Measured intensity at 975 Å as a function of galactic latitude. The present observations are indicated by their corresponding letter. The calculation from Henry (1977) for similar directions (but for a much larger field) are shown by triangles. A latitude dependence calculated by Gondhalekar and Wilson (1975) for the band 975–1025 Å is shown by the solid line.

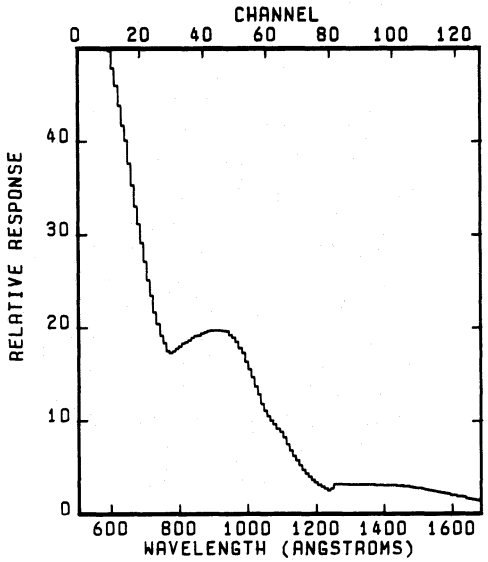

FIG. 7.—Relative spectral response of the *Voyager 2* UV instrument, in photon units.

970 Å, where it abruptly takes on a lower slope toward larger wavelengths. The abrupt change in slope at 970 Å is most easily observed in Figure 3, from which the Lβ 1026 Å emission has been removed. The instrumental response to a step function at 912 Å would produce a change in slope at 878 Å and 946 Å. The results seem to suggest that, although we have a declining spectral brightness toward shorter wavelengths, there is an abrupt termination of measurable signal below about 912 Å, extending to 770 Å. Figure 7 shows that the sensitivity of the instrument does not change markedly over this wavelength region. The "background" spectrum of Figure 1*d* appears to have the same characteristic. This spectrum also contains an apparent measurable continuum beginning abruptly at 770 Å extending to shorter wavelengths, with a brightness of 2.6×10^{-8} ergs $(cm^2\ s\ sr\ Å)^{-1}$ at 750 Å. The emission in this region is statistically significant and varies relative to other regions of the spectrum; the brightness at 750 Å in Figure 4 is 10^{-8} ergs $(cm^2\ s\ sr\ Å)^{-1}$, reduced by a factor of about 2.6 relative to the "background" spectrum. Determination of the origin of this emission will require a larger set of analyzed data. In any case, the appearance of a sharp edge in the emission spectrum at about 912 Å seems to indicate the presence of a sufficient abundance of neutral hydrogen atoms in the vicinity of the solar system to remove the interstellar EUV radiation down to at least 770 Å. Observations of resonance scattering of solar radiation by the interstellar medium suggest an H I number density of 0.04 cm^{-3} in the near vicinity of the solar system (Ajello 1978). On this basis, most of the radiation in the 912–1150 Å region observed by the *Voyager* instrument must originate beyond a range of 5 pc (see Grewing 1975; Paresce and Bowyer 1976).

The 1250–1680 Å region in the two spectra that have been reduced by application of the scattering matrix (Figs. 1*d*, 2*d*) shows no significant variation in absolute intensity or spectral content. The spectrum contains some well-defined structure with features at about 1320, 1400, 1530, and 1630 Å. The independence of the emission from the 1216 Å feature is demonstrated by the fact that it appears in the spectrum of Figure 3. The origin of this emission requires further investigation, since it is not clear that it is extragalactic. Measurements by Henry *et al.* (1977) at the galactic poles indicate an extragalactic component of ~300 photons $(cm^2\ s\ sr\ Å)^{-1}$ at 1400 Å, about 60 times less bright than the spectrum of Figure 4.

The observations analyzed here were made at galactic latitudes less than 45° and therefore were not optimum for detecting radiation whose origin is outside the Galaxy. The more sophisticated data-analysis techniques described briefly in § II with results shown in Figures 1*d* and 2*d* combined with observations specifically aimed at searching for cosmic EUV radiation are expected to remove these difficulties in the future. More complete information on the dependence of intensity on galactic latitude should become available as well.

This work was supported by the Jet Propulsion Laboratory, California Institute of Technology, under NASA contract NAS 7-100.

REFERENCES

Ajello, J. M. 1978, *Ap. J.*, **222**, 1068.
Belyaev, V. P., Kurt, V. G., Melioranskii, A. S., Smirnov, A. S., Sorokin, L. S., and Tiit, V. M. 1970, *Cosmic Res.*, **8**, 677.
Broadfoot, A. L., and Sandel, B. R. 1977, *Appl. Optics*, **16**, 1533.
Broadfoot, A. L., *et al.* 1977, *Space Sci. Rev.*, **21**, 183.
Davidsen, A., Bowyer, S., and Lampton, M. 1974, *Nature*, **247**, 513.
Gondhalekar, P. M., and Wilson, R. 1975, *Astr. Ap.*, **38**, 329.
Grewing, M. 1975, *Astr. Ap.*, **38**, 391.
Hayakawa, S., Yamashita, K., and Yoshioka, S. 1969, *Ap. Space Sci.*, **5**, 493.
Henry, R. C. 1973, *Ap. J.*, **179**, 97.
———. 1977, *Ap. J. Suppl.*, **33**, 451.
Henry, R. C., Swandic, J. R., Shulman, S. D., and Fritz, G. 1977, *Ap. J.*, **212**, 707.
Hill, J. K., and Silk, J. 1975, *Ap. J.*, **198**, 299.
Jura, M. 1974, *Ap. J.*, **191**, 375.
Paresce, F., and Bowyer, S. 1976, *Ap. J.*, **207**, 432.
Sandel, B. R., Shemansky, D. E., and Broadfoot, A. L. 1978, *Nature*, in press.
Shemansky, D. E., Sandel, B. R., and Broadfoot, A. L. 1978, *J. Geophys. Res.*, in press.

A. Lyle Broadfoot: Kitt Peak National Observatory, P.O. Box 26732, Tucson, AZ 85726

B. R. Sandel and D. E. Shemansky: *Voyager* Program, 3625 East Ajo Way, Tucson, AZ 85713